ELSEVIER

Electroencephalography and clinical Neurophysiology 103 (1997) 386–394

Spatial filter selection for EEG-based communication

Dennis J. McFarland*, Lynn M. McCane, Stephen V. David, Jonathan R. Wolpaw

Wadsworth Center for Laboratories and Research, New York State Department of Health, P.O. Box 509, Empire State Plaza, Albany, NY 12201-0509, USA

Accepted for publication: 3 March 1997

Abstract

Individuals can learn to control the amplitude of mu-rhythm activity in the EEG recorded over sensorimotor cortex and use it to move a cursor to a target on a video screen. The speed and accuracy of cursor movement depend on the consistency of the control signal and on the signal-to-noise ratio achieved by the spatial and temporal filtering methods that extract the activity prior to its translation into cursor movement. The present study compared alternative spatial filtering methods. Sixty-four channel EEG data collected while well-trained subjects were moving the cursor to targets at the top or bottom edge of a video screen were analyzed offline by four different spatial filters, namely a standard ear-reference, a common average reference (CAR), a small Laplacian (3 cm to set of surrounding electrodes) and a large Laplacian (6 cm to set of surrounding electrodes). The CAR and large Laplacian methods proved best able to distinguish between top and bottom targets. They were significantly superior to the ear-reference method. The difference in performance between the large Laplacian and small Laplacian methods presumably indicated that the former was better matched to the topographical extent of the EEG control signal. The results as a whole demonstrate the importance of proper spatial filter selection for maximizing the signal-to-noise ratio and thereby improving the speed and accuracy of EEG-based communication. © 1997 Elsevier Science Ireland Ltd.

Keywords: Prosthesis; Rehabilitation; Assistive communication; Operant conditioning; Sensorimotor cortex; Mu rhythm; Electroencephalography

1. Introduction

1.1. EEG-based communication

Many people with severe motor disabilities require alternative methods for communication and control. Over the past decade, a number of studies have evaluated the possibility that scalp-recorded EEG activity might be the basis for a new alternative communication channel (Wolpaw et al., 1986, 1991; Farwell and Donchin, 1988; Sutter, 1992; McFarland et al., 1993; Pfurtscheller et al., 1993; Wolpaw and McFarland, 1994).

EEG-based communication systems measure specific components of EEG activity and use the results as a control signal. In some systems, these components are potentials evoked by stereotyped sensory stimuli (e.g. visual (Farwell and Donchin, 1988; Sutter, 1992)). Other systems, including the one employed in the present study, use EEG components that are spontaneous in the sense that they are not dependent on specific sensory events. Our system uses the mu rhythm, an 8–12 Hz rhythm recorded from the scalp over somatosensory cortex, and/or closely related higher frequency components recorded from the same region (Wolpaw et al., 1986, 1991; McFarland et al., 1993; Wolpaw and McFarland, 1994). Pfurtscheller et al. (1993) employ EEG features defined by neural network analyses.

In our system, signals extracted from the EEG control movement of a cursor on a video screen. Two factors determine the accuracy and speed of cursor movement, i.e. the skill of the subject, that is, the magnitude and consistency of the control signals that the subject produces and the signal-to-noise ratio achieved by the online analysis that extracts these control signals from the EEG and translates them into cursor movement. The noise has two sources: non-EEG artifacts including EMG, EKG, and eye movement and eyeblink potentials; and non-mu EEG components such as the visual alpha rhythm.

* Corresponding author.

PII S0013-4694(97)00022-9

EEG 96031

1.2. Signal enhancement and noise reduction by temporal and spatial filtering

Both classes of noise differ from the control signal in their topographical and/or frequency distributions. The mu rhythm control signal is an 8–12 Hz component that is focused over sensorimotor cortex. In contrast, for example, EMG has a wide frequency range, is maximal at higher frequencies (>30 Hz), and is not sharply focused over sensorimotor cortex; eye-movement activity also has a wide frequency range, is maximal at low frequencies (<5 Hz), and is most prominent over anterior head regions; and the visual alpha rhythm, while it may extend to central scalp regions, is most prominent over the parieto-occipital cortex (Salenius et al., 1995; McFarland et al., 1997, in press). Spatial and temporal filtering methods can increase the signal-to-noise ratio by enhancing the control signal and/or reducing noise.

The present study addresses the problem of selecting the best spatial filtering method. Clearly, the proper selection is determined by the location and extent of the control signal (e.g. the mu rhythm) and the locations and extents of the various sources of EEG or non-EEG noise. Noise sources are complex and highly variable both across and within subjects. Thus, spatial filter selection is best effected by determining which filter actually provides the highest signal-to-noise ratio, and therefore is likely to support the most accurate and rapid cursor movement. The present study compares four alternative methods (a conventional ear reference, a common average reference (CAR) and two different Laplacian derivations).

In the CAR, the average value of the entire electrode montage (the common average) is subtracted from that of the channel of interest. If the entire head is covered by equally spaced electrodes and the potential on the head is generated by point sources, the CAR results in a spatial voltage distribution with a mean of zero (Bertrand et al., 1985). While the assumptions of uniform and complete electrode coverage and point sources are usually not met completely in practice, the CAR provides EEG recording that is nearly reference-free. Because it emphasizes components that are present in a large proportion of the electrode population, the CAR reduces such components and thereby functions as a high-pass spatial filter (it accentuates components with highly focal distributions) (Nunez et al., 1994). Conversely, components that are present in most of the electrode population but absent or minimal in the electrode of interest may appear as 'ghost potentials' in CAR recordings (Desmedt et al., 1990).

The Laplacian method calculates for each electrode location the second derivative of the instantaneous spatial voltage distribution, and thereby emphasizes activity originating in radial sources immediately below the electrode (Zhou, 1993; Nunez, 1995). Thus, it is a high-pass spatial filter that accentuates localized activity and reduces more diffuse activity. High spatial resolution can be achieved by using many electrodes (e.g. 64) spread over the entire scalp. The value of the Laplacian at each electrode location is calculated by combining the value at that location with the values of a set of surrounding electrodes. The distances to the set of surrounding electrodes determine the spatial filtering characteristics of the Laplacian. As distance decreases, the Laplacian becomes more sensitive to potentials with higher spatial frequencies and less sensitive to those with lower spatial frequencies. The present study keeps electrode location and number (i.e. 64) constant and evaluates Laplacians calculated with two different sets of surrounding electrodes, namely nearest-neighbor (adjacent) electrodes (a small Laplacian) and next-nearest-neighbor electrodes (a large Laplacian). If the control signal is highly localized and if that localization is stable over time, we would expect the small Laplacian to give a higher signal-to-noise ratio. On the other hand, if the control signal is less highly localized and/or varies in exact location over time, we would expect the large Laplacian to prove superior.

2. Methods

The subjects were 4 adults (1 female and 3 male, ages 29, 30, 40 and 66). Three were healthy, while the oldest had early-stage amyotrophic lateral sclerosis, manifested throughout the time of study only by mild weakness in one leg. All gave informed consent for the study, which had been reviewed and approved by the New York State Department of Health Institutional Review Board. After an initial evaluation had defined the frequencies and scalp locations of mu rhythm activity and related beta rhythm activity, each subject participated in 26–86 1-h sessions at a rate of 1–3 sessions per week. The overall purpose of these lengthy study periods was to maximize each subject's performance through practice and through improvements in the online system. Over the course of each subject's sessions, offline data evaluations and concurrent improvements in the hardware and software capabilities of the online system led to adjustments in the electrode locations, referencing method and frequency analysis used in the online algorithm that controlled cursor movement. The next section describes the final online methodology that was used in all subjects.

2.1. Online performance and data collection

Each subject sat in a reclining chair facing a video screen and was asked to remain motionless during performance. Scalp electrodes recorded 64 channels of EEG (Fig. 1) (Sharbrough et al., 1991), each referring to a reference electrode on the right ear (amplification 20 000; bandpass 1–35 Hz). A subset of channels were digitized at 196 Hz and used to control cursor movement online as described below. In addition, all 64 channels were digitized at 128 Hz and stored for later analysis.

This study examined EEG control of one-dimensional

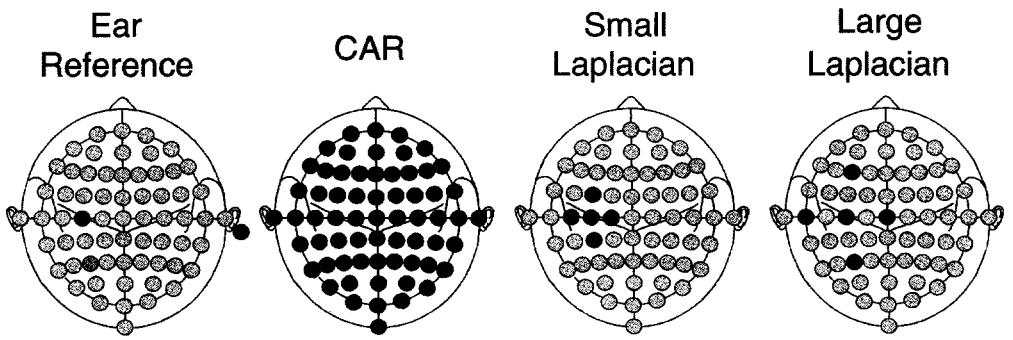

Fig. 1. Electrode locations used in the application of each spatial filter method to the activity recorded from C3 (red). During data acquisition, all electrodes are referred to the ear reference. For the CAR and Laplacian methods, the activity at the green electrodes is averaged and subtracted from the activity at C3.

(vertical) cursor movement. Cursor movement was controlled as follows. After digitization, two EEG channels, one over sensorimotor cortex of each hemisphere (e.g. C3 and C4), were re-referenced to a common average reference (CAR) composed of 19 electrodes distributed over the entire scalp (i.e. the electrodes of the 10–20 system (Jasper, 1958)). This 19-channel CAR, used to increase the speed of online analysis, provided an EEG signal equivalent to that from a full 64-channel CAR (in offline analysis, the signals provided by the 19-electrode CAR and the 64-electrode CAR were very highly correlated ($r = +0.99$)). Every 100 ms, the most recent 200-ms segment from each channel was analyzed by an autoregressive algorithm (Marple, 1987), and the square root of power in a 4 or 5-Hz wide frequency band centered at 10, 12 or 20 Hz was calculated (Subject A, 18–22 Hz; B, 7.5–12.5 Hz; C, 17.5–22.5 Hz; D, 10–14 Hz). (These frequency components encompass the arch-shaped mu rhythm or the central beta rhythm, both of which are generated in sensorimotor cortex (Gastaut, 1952; Kuhlman, 1978; Pfurtscheller and Berghold, 1989; Pfurtscheller et al., 1997, in press).) The sum of the results from the two channels was the independent variable in a linear equation that defined a vertical cursor movement. The movement was in units of cursor steps. A positive value caused upward movement and a negative value caused downward movement. Thus, every 100 ms, the cursor moved the defined number of steps up or down the screen. The intercept of the equation was set so that if future performance was similar to previous performance the net cursor movement over all trials would be zero (Wolpaw et al., 1991; McFarland et al., 1993; Wolpaw and McFarland, 1994). Thus, the intercept reduced bias in one direction or another and maximized the influence that the subject's EEG control had on the direction (upward or downward) of cursor movement. The slope was set on the basis of previous performance so that the average duration of cursor movement would be about 2 s.

Each subject participated in 1–3 training sessions per week. In each session, one-dimensional cursor control was practiced in eight runs of 3 min each, separated by 1-min breaks. A run consisted of a series of trials. Each trial began with a 1-s period during which the screen was blank. Then, a target appeared at the top or bottom edge of the screen. One second later, the cursor appeared in the center of the screen and began to move vertically 10 times/s according to the linear equation described above. The distance from the top to the bottom of the screen was 188 cursor steps (the cursor's initial position was 94 steps from the top and 94 steps from the bottom). The subject's task was to move the cursor to the target. The trial ended when the cursor touched the top or bottom edge. When it touched the correct edge, the target flashed for 1 s as a reward and the computer registered a hit. When it touched the other edge, the target disappeared, the cursor remained fixed on the screen for 1 s, and the computer registered a miss. In either case, the next trial then began with 1 s of blank screen. Equal numbers of top and bottom targets appeared in an order randomized in blocks of eight, and a miss did not cause the target to be repeated. Thus, accuracy expected in the absence of any EEG control was 50%.

2.2. *Offline analysis*

The goal of analysis was to compare the four different spatial filtering methods with regard to their ability to distinguish top targets from bottom targets, that is, in regard to the prominence of the difference in control signal values between EEG recorded during top targets and EEG recorded during bottom targets. To do this, we analyzed 64-channel EEG data from four sessions from each of the four subjects. These sessions were near the end of training, so that each subject had a high level of EEG control (≥90% accuracy).

Since the 64 electrode locations had been digitized sequentially over 7.8 ms (digitization rate of 128 Hz) and the Laplacian and CAR waveforms were derived by combining multiple electrodes, the data were temporally aligned by linear interpolation prior to processing. Then, for each electrode location, we derived the EEG waveform by each of the four methods, i.e. ear reference, CAR (using all 64 electrodes as the reference), small Laplacian (nearest-neighbor) and large Laplacian (next-nearest-neighbor). Fig. 1 illustrates the derivation of these waveforms for electrode C3 over left sensorimotor cortex.

The CAR was computed according to the formula,

$$V_i^{CAR} = V_i^{ER} - 1/n \sum_{j=1}^{n} V_j^{ER}$$

where V_i^{ER} is the potential between the ith electrode and the reference and n is the number of electrodes in the montage (i.e. 64).

To calculate the Laplacian derivations, we used a finite difference method, which approximates the second derivative by subtracting the mean activity at surrounding electrodes from the channel of interest. The Laplacian was computed according to the formula,

$$V_i^{LAP} = V_i^{ER} - \sum_{j \epsilon Si} g_{ij} V_j^{ER}$$

where

$$g_{ij} = 1/d_{ij} / \sum_{j \epsilon Si} 1/d_{ij}$$

Si is the set of electrodes surrounding the ith electrode, and d_{ij} is the distance between electrodes i and j (where j is a member of Si). Fig. 1 shows examples of these sets. For the small Laplacian, Si was the set of nearest-neighbor electrodes. For the large Laplacian, it was the set of next-nearest-neighbor electrodes. Thus, in the central head regions of greatest importance, each electrode was at the center of a square and the four Si electrodes were at the corners. In these regions, the distance from the ith electrode to each surrounding electrode (d_{ij}) was 3 cm for the small Laplacian and 6 cm for the large Laplacian. For locations near the edges of the 64-channel montage, the Si electrodes were selected as suggested by Zhou (1993).

The waveforms resulting from each of these methods were then subjected to an autoregressive spectral analysis (maximum entropy method (MEM) (Marple, 1987)). The results were evaluated in terms of voltage values for top versus bottom targets, and also in terms of the values of r^2 for the top/bottom comparison. This latter measure is the proportion of variance of the EEG voltages that is accounted for by target location (Winer, 1971). Thus, r^2 reflects the signal-to-noise ratio. These analyses are presented here as frequency spectra for voltage and r^2 at the electrode locations over sensorimotor cortex that controlled cursor movement online, and as scalp topographies for voltage and r^2 at the frequencies used for online control (e.g. 12 Hz).

3. Results

3.1. Waveforms

Fig. 2 shows, for a single top target trial and a single bottom target trial of one subject, the C3 waveforms provided by each of the four spatial filter methods. For each trial, the top trace in each of the three columns is the C3 ear-referenced waveform. The middle traces are the reference waveforms calculated from the sets of neighboring electrodes (shown in Fig. 1) by the equations given above. The bottom traces are the CAR, small Laplacian and large Laplacian waveforms at C3 derived by subtracting the calculated reference waveform from the ear-referenced waveform. The arrows indicate target appearance, beginning of cursor movement and target hit. The EKG artifacts (asterisks) visible in the ear-referenced waveforms are absent or minimal in the CAR, small Laplacian and large Laplacian waveforms. Most importantly, the 7.5–12.5 Hz mu rhythm, the signal that controlled cursor movement online, and the effect of target appearance on it, are most evident in the CAR and large Laplacian derivations. In the top target trial, the rhythm becomes much more prominent about 0.5 s after the target appears, while in the bottom target trial, it largely disappears 0.5 s after the target appears. The mu rhythm and the effect of target appearance are much less evident in the small Laplacian derivation, and barely apparent in the ear-referenced waveform.

3.2. Effectiveness of spatial filter methods

Fig. 3 summarizes, for all subjects and sessions, the data from the locations (e.g. C3 and C4) that controlled cursor movement online. It shows average voltage and r^2 frequency spectra for each spatial filter method. With each method, the voltage difference between top and bottom targets and the corresponding r^2 value is focused at 11 Hz and 21 Hz (the frequencies that controlled cursor movement online). However, the magnitude of the difference between top and bottom targets and the signal-to-noise ratio achieved by that difference (represented by r^2) varies markedly across methods. The CAR and large Laplacian methods achieve the best results, the small Laplacian is next, and the ear reference gives the poorest result.

Table 1 shows, for each subject and each method, the average values of r^2 for the locations and frequency used online. As in the average data of >Fig. 3, values are uniformly highest and similar for the CAR and large Laplacian, intermediate for the small Laplacian and smallest for the ear reference. An analysis of variance revealed a significant effect of method ($F = 16.31$, d.f. = 3/9, $P < 0.001$), and a Newman–Keuls test indicated that the CAR and large Laplacian values were significantly larger than the ear-reference values ($P < 0.05$ in each case).

Fig. 4 displays for each method the average voltage topographies for top targets and bottom targets and the corresponding r^2 topographies for all subjects and sessions at the frequencies used online. With each method, the voltage is greater for top targets than for bottom targets, and the maximum voltages are near or at the locations used to control cursor movement online (i.e. over one or both sensorimotor cortices). Furthermore, all four r^2 topographies indicate that the difference between top and bottom targets (i.e. the subjects' EEG control) is also focused over sensorimotor cortices. At the same time, the values of r^2 are highest for the CAR and large Laplacian methods, smaller for the small

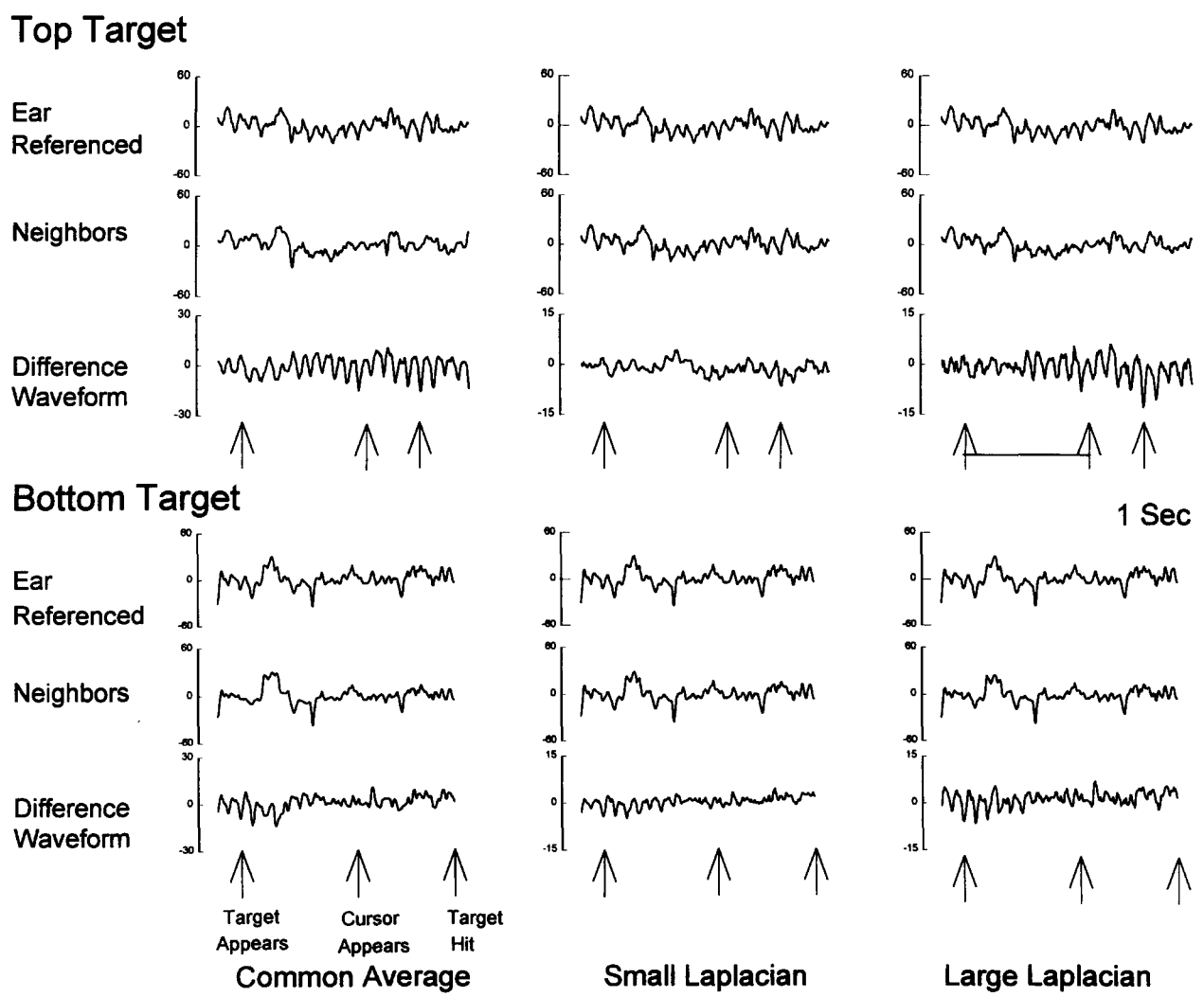

Fig. 2. Derivation of the C3 waveforms for a single top target trial and a single bottom target trial for each of the four spatial filter methods. The top trace in each column is the C3 ear-referenced waveform. The middle traces are the averages of the ear-referenced activity from the different sets of surrounding electrodes (the green locations in Fig. 1). The bottom traces are the CAR, small Laplacian and large Laplacian waveforms at C3 obtained by subtracting the average of the surrounding electrodes from the C3 ear-referenced waveform. Asterisks mark the EKG in the ear-referenced waveform.

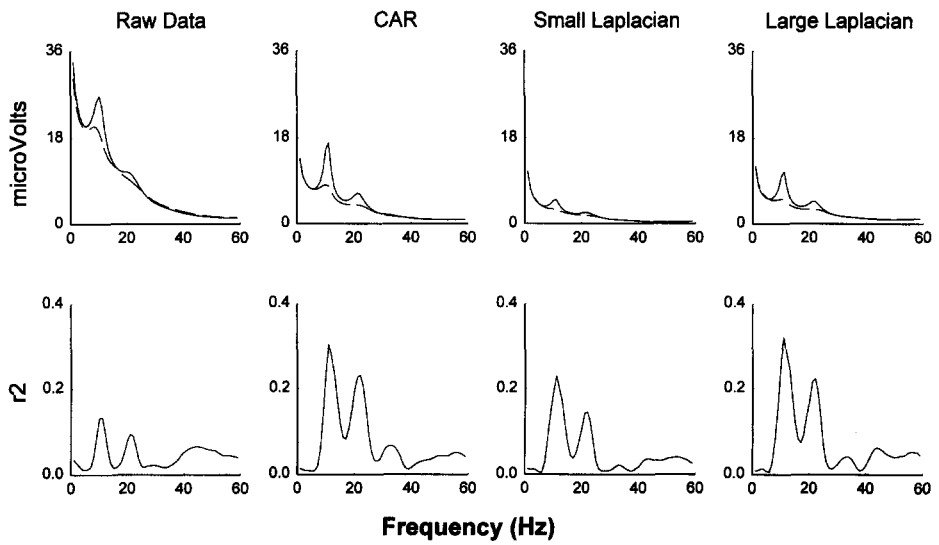

Fig. 3. Average voltage spectra for top targets (solid lines) and bottom targets (dashed lines) and average spectra of r^2 for the top/bottom difference for all sessions of all subjects for the locations that controlled cursor movement online.

Table 1

Average r^2 values for each spatial filtering method at the end of training

Subject	Ear reference	CAR	Small Laplacian	Large Laplacian
A	0.34	0.48	0.37	0.48
B	0.10	0.31	0.19	0.29
C	0.10	0.47	0.31	0.48
D	0.26	0.42	0.34	0.41
All	0.21	0.42	0.30	0.41

Laplacian, and smallest for the ear-reference method.

3.3. Effectiveness prior to CAR training

As indicated in Section 2, all subjects were switched to the CAR online algorithm early in their training (after 11–28 sessions). Thus, the final superiority of the CAR and large Laplacian methods (Table 1) could conceivably be a result of training. To evaluate this possibility, we also analyzed sessions conducted before subjects were switched to the CAR algorithm. Two subjects began training with an ear-reference algorithm, and two began with the bipolar algorithm used in our initial studies (with electrodes 3 cm anterior and posterior to C3) (Wolpaw et al., 1991). All four had reached accuracies of 70–80% by the time they were switched to the CAR algorithm.

Using the data from these pre-CAR sessions, we evaluated the effectiveness of the different spatial filters. Table 2 shows, for each subject and each method, the average values of r^2 for the same locations and frequency evaluated in Table 1 (i.e. those used subsequently for training with the CAR algorithm). Just as for the final CAR sessions analyzed in Table 1, values are highest and similar for the CAR and large Laplacian, intermediate for the small Laplacian, and smallest for the ear reference. With the higher variance of these early data, the effect of method was of borderline significance ($P = 0.06$). Nevertheless, the same differences noted in Table 1 appear to be present here as the CAR and large Laplacian values are higher than the ear reference values. Thus, the superiority of the CAR and large Laplacian methods apparent in Table 1 is probably not attributable simply to subject training.

3.4. The impact of temporal alignment

During system operation, the 64 ear-referenced EEG channels are sampled sequentially rather than simulta-

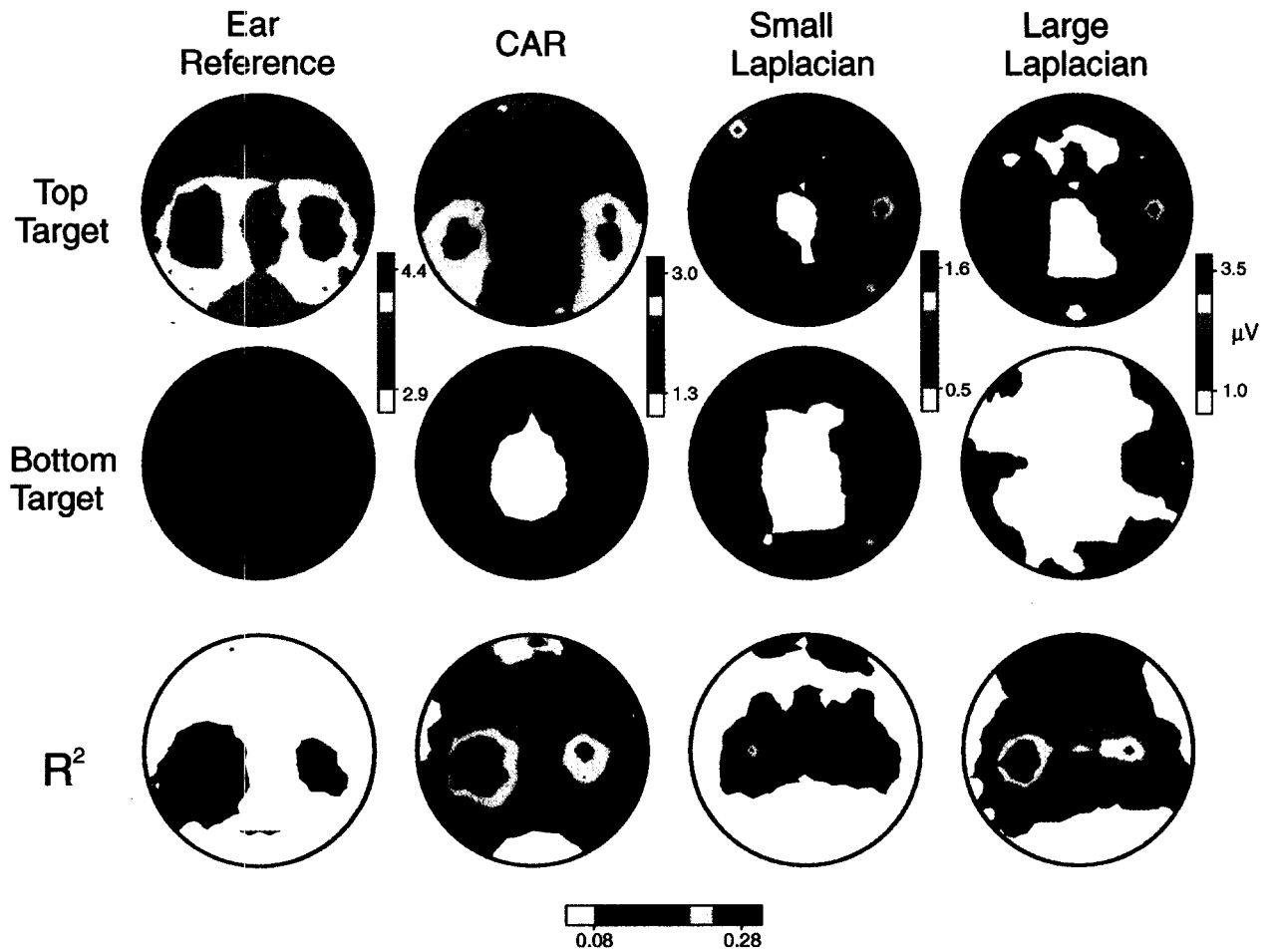

Fig. 4. Average voltage topographies for top targets and bottom targets and average spectra of r^2 for the top/bottom difference for all sessions of all subjects.

Table 2

Average r^2 values for each spatial filtering method early in training

Subject	Ear reference	CAR	Small Laplacian	Large Laplacian
A	0.18	0.33	0.17	0.34
B	0.22	0.26	0.13	0.27
C	0.20	0.28	0.30	0.29
D	0.03	0.10	0.12	0.12
All	0.16	0.24	0.18	0.25

neously. Because each point in the Laplacian waveform (and the CAR waveform) is derived from multiple electrodes, the inter-electrode phase differences caused by this sequential sampling introduce noise into the Laplacian waveform (and to a lesser extent into the CAR waveform). For example, a signal that is identical in amplitude and phase at all five electrodes of the Laplacian derivation (i.e. the electrode of interest and its four nearest or next-nearest neighbors), and should therefore be completely eliminated from the Laplacian waveform, is not completely eliminated. Its remnant constitutes noise in the Laplacian waveform and in the frequency spectrum derived from that waveform. The magnitude of the noise depends on the time required to sample all five electrodes and on the frequency of the signal. In the present case, the maximum sampling time is 5.1 ms for the online data (196 Hz) and 7.8 ms for the offline data (128 Hz), and the signals of greatest interest are in the range of 1–30 Hz.

Fig. 5 illustrates the impact of sequential sampling. It shows large Laplacian voltage and r^2 spectra from a single subject and session calculated offline. The spectra on the top were calculated without aligning the samples from the different electrodes, while those on the bottom were calculated after the samples were aligned by linear interpolation. The voltage difference between top and bottom targets is absolutely and relatively larger and the r^2 value is higher with sample alignment. As expected, the effect of alignment is greater for the higher-frequency beta rhythm than for the lower-frequency mu component. Nevertheless, it is substantial for both. The r^2 value is 44% higher with alignment for the mu component and 337% higher for the beta component. Results of this type indicate that temporal alignment of the samples from different electrodes can substantially improve the signal-to-noise ratio achieved by spatial filters that operate by combining samples from multiple electrodes.

4. Discussion

The results summarized in Table 1 show that for each of these well-trained subjects, the CAR and large Laplacian methods provide a better signal-to-noise ratio for mu-rhythm or beta-rhythm based cursor control than does the standard ear-reference method. Furthermore, the additional analysis of early data provided in Table 2 suggests that the superiority of the CAR and large Laplacian methods cannot be ascribed to the fact that the subjects were exposed to the CAR method during training. These methods are also superior for data obtained prior to CAR exposure.

The CAR and Laplacian methods are superior to the ear reference method presumably because they are high-pass spatial filters and thus enhance focal activity from local sources (e.g. the mu rhythm and closely related beta activity) and reduce widely distributed activity, including that from distant sources (e.g. EMG, eye movements and blinks, visual alpha rhythm). The performance (signal-to-noise ratio) of these methods relative to each other depends on the topographical size of the mu or beta rhythm control signal (i.e. on its spatial frequency) and also on the topographical sizes and locations of the various noise signals (both EEG and non-EEG). The identities and characteristics of the various noise signals are incompletely defined and presumably vary considerably both across and within individuals. The impact on performance of the spatial frequency of the control signal is more readily estimated.

Fig. 6 illustrates the band-pass characteristics of the spatial filters used in the present study. It shows each filter's values for a signal, the amplitude of which varies as a complex sinusoid from +1 to −1 across the scalp. The spatial frequency of the signal, i.e. the distance on the scalp between adjacent positive (or negative) amplitude peaks,

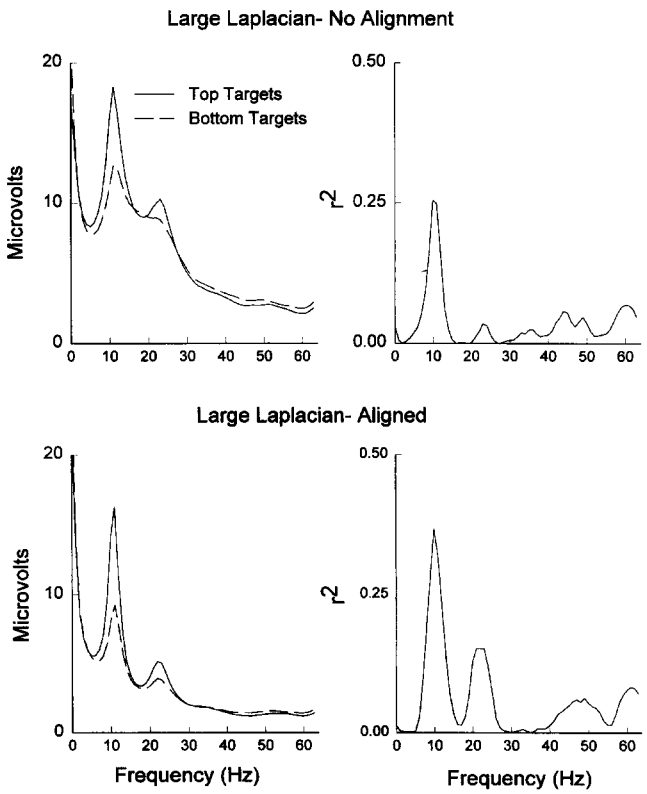

Fig. 5. Large Laplacian voltage spectra for top targets (solid lines) and bottom targets (dashed lines) and average spectra of r^2 from one session of one subject calculated with (right) and without (left) linear interpolation to correct for phase differences caused by the sequential digitization of channels.

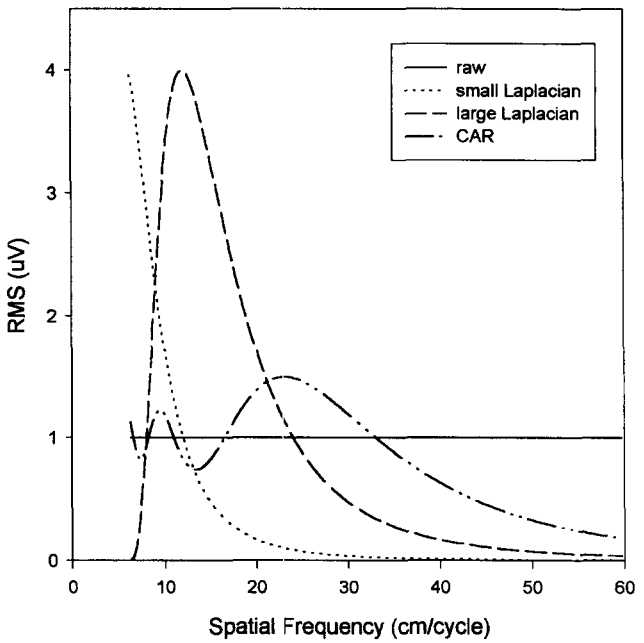

Fig. 6. Spatial band-pass characteristics of the spatial filter methods used in the present study. Each trace shows for a given method the square root of the rms values (amplitude in microvolts) of a signal that varies sinusoidally in amplitude across the scalp as its spatial frequency varies from 6 cm, twice the interelectrode distance in the present study (the highest spatial frequency that would not cause spatial aliasing), to 60 cm (the approximate circumference of the head).

is given on the *X*-axis. It varies from 6 cm (the minimum distance at which spatial aliasing will not occur with our interelectrode distance of 3 cm) to 60 cm (approximately the circumference of the head). The *Y*-axis shows, for each filter method of the present study, the square root of the root-mean-square (rms) value as a function of spatial frequency. The ear reference is unaffected by spatial frequency and gives a value of +1 for all frequencies. The small Laplacian is most sensitive to high spatial frequencies and gives the highest amplitude for frequencies near 6 cm. The large Laplacian responds best to spatial frequencies near 12 cm and the CAR is most sensitive to even lower spatial frequencies. It gives the highest amplitude for a frequency of 23 cm. If the diameter of the scalp distribution of an EEG control signal is equated to half the period of a sinusoid, then Fig. 6 suggests that the small Laplacian would be most sensitive to a control signal with a diameter of about 3 cm, the large Laplacian would be most sensitive to a control signal with a distribution diameter of about 6 cm and the CAR would be most sensitive to a control signal with a distribution diameter of about 12 cm.

The putative source of the mu and beta rhythm control signals, the sensorimotor cortex, is an extended sheet of tissue lying on the surface of the hemisphere largely parallel to the scalp. While the spatial extent of the area of cortex responsible for the control signal is unknown, the size of the sensorimotor cortex and the area of control evident in the ear reference topographies (e.g. Fig. 4) suggest that the control signal has a diameter on the scalp of at least 6 cm. A diameter of 6–12 cm would be consistent with the observed superiority of the large Laplacian and CAR methods. Nevertheless, as noted above, the relative performance of the different methods is also a function of the locations and extents of the noise sources, which are not precisely known.

Two other factors may conceivably have contributed to the superiority of the large Laplacian method. First, as the distances between the electrodes used in calculation of the Laplacian for each electrode location decrease, the differences between the values of the recorded signal also decrease. At some point, measurement noise and/or the finite resolution of analog-to-digital conversion begin to obscure the control signal (Schwab, 1988). Second, even if the spatial extent of the control signal is small, it may vary in location between trials or even within trials, and thus it may often fall outside the highly localized detection focus that the small Laplacian method creates for each electrode location. Furthermore, unavoidable inter-session variability in placement of the electrode cap (±0.5 cm) might also contribute to placing the source outside the focus of the small Laplacian method.

The CAR and Laplacian methods described here are easily implemented in real-time with standard digital signal processing hardware. The results illustrated in Fig. 5 indicate that online implementation of these methods should include temporal alignment to eliminate the noise introduced by sequential sampling of the electrode locations. More elaborate Laplacian methods are available (e.g. fitting the instantaneous spatial potential values with a cubic spline function or some other interpolating function (Zhou, 1993; Nunez et al., 1994)). However, because these procedures involve non-linear curve fitting, they are computationally intensive and may not as yet be practical for online operation. Furthermore, the question of whether such methods are likely to provide results superior to those of the simpler method used here has yet to be evaluated by comparisons like those of the present study.

Finally, while the CAR and large Laplacian appear to be well-suited for a communication system using the mu rhythm or closely related beta activity, they would not necessarily be appropriate for systems using more broadly distributed activity, such as the P300 system described by Farwell and Donchin (1988). For each system, the spatial filter chosen should maximally accentuate the control signal and maximally attenuate other EEG activity and non-EEG artifacts.

Acknowledgements

This work was supported in part by the National Center for Medical Rehabilitation Research of the National Institute of Child Health and Human Development (Grant HD30146).

References

Bertrand, O., Perrin, F. and Pernier, J. A theoretical justification of the average reference in topographic evoked potential studies. Electroenceph. clin. Neurophysiol., 1985, 62: 462–464.

Desmedt, J.E., Chalklin, V. and Tomberg, C. Emulation of somatosensory evoked potential (SEP) components with the 3-shell head model and the problem of 'ghost potential fields' when using an average reference in brain mapping. Electroenceph. clin. Neurophysiol., 1990, 77: 243–258.

Farwell, L.A. and Donchin, E. Taking off the top of your head: toward a mental prosthesis utilizing event-related brain potentials. Electroenceph. clin. Neurophysiol., 1988, 70: 510–523.

Gastaut, H. Etude electrocorticographique de la reactivite des rythmes rolandiques. Rev. Neurol., 1952, 87: 176–182.

Jasper, H.H. The ten-twenty electrode system of the International Federation. Electroenceph. clin. Neurophysiol., 1958, 10: 371–375.

Kuhlman, W.N. Functional topography of the human mu rhythm. Electroenceph. clin. Neurophysiol., 1978, 44: 83–93.

Marple, S.L. Digital Spectral Analysis. Prentice Hall, London, 1987.

McFarland, D.J., Lefkowicz, A.T. and Wolpaw, J.R. Design and operation of an EEG-based brain-computer interface (BCI) with digital signal processing technology. Behav. Res. Methods, Instrum. Comput., 1997, in press.

McFarland, D.J., Neat, G.W., Read, R.F. and Wolpaw, J.R. An EEG-based method for graded cursor control. Psychobiology, 1993, 21: 77–81.

Nunez, P.L. Neocortical Dynamics and Human EEG Rhythms. Oxford University Press, New York, 1985.

Nunez, P.L., Silberstein, R.B., Cadusch, P.J., Wijesinghe, R.S., Westdorp, A.F. and Srinivasan, R. A theoretical and experimental study of high resolution EEG based on surface Laplacians and cortical imaging. Electroenceph. clin. Neurophysiol., 1994, 90: 40–57.

Pfurtscheller, G. and Berghold, A. Patterns of cortical activation during planning of voluntary movement. Electroenceph. clin. Neurophysiol., 1989, 72: 250–258

Pfurtscheller, G., Flotzinger, D. and Kalcher, J. Brain-computer interface: a new communication device for handicapped persons. J. Microcomput. Applic., 1993, 16: 293–299.

Pfurtscheller, G., Neuper, C. and Berger, J. Source localization using event-related desynchronization (ERD) within the alpha band. Brain Topogr., 1994, 6: 269–275.

Pfurtscheller, G., Pregenzer, M. and Neuper, C. Visualization of sensorimotor areas involved in preparation for hand movement based on classification of alpha and beta band activity in single EEG trials in man. Neurosci. Lett., 1997, in press.

Salenius, S., Kajola, M., Thompson, W.L., Kosslyn, S. and Hari, R. Reactivity of magnetic parieto-occipital alpha rhythm during visual imagery. Electroenceph. clin. Neurophysiol., 1995, 95: 453–462.

Schwab, A.J. Field Theory Concepts: Electromagnetic Fields, Maxwell's Equations, Grad, Curl, Div, etc. Springer-Verlag, Berlin, 1988.

Sharbrough, F., Chatrian, G.E., Lesser, R.P., Luders, H., Nuwer, M. and Picton, T.W. American Electroencephalographic Society guidelines for standard electrode position nomenclature. J. Clin. Neurophysiol., 1991, 8: 200–202.

Sutter, E.E. The brain-response interface: communication through visually guided electrical brain responses. J. Microcomput. Applic., 1992, 15: 31–45.

Winer, B.J. Statistical Principles in Experimental Design. McGraw-Hill, New York, 1971.

Wolpaw, J.R. and McFarland, D.J. Multichannel EEG-based brain-computer communication. Electroenceph. clin. Neurophysiol., 1994, 90: 444–449.

Wolpaw, J.R., McFarland, D.J. and Cacace, A.T. Preliminary studies for a direct brain-to-computer interface. In: Projects for Persons with Disabilities. IBM Technical Symposium, 1986, pp. 11–20.

Wolpaw, J.R., McFarland, D.J., Neat, G.W. and Forneris, C.A. An EEG-based brain-computer interface for cursor control. Electroenceph. clin. Neurophysiol., 1991, 78: 252–259.

Zhou, P. Numerical Analysis of Electromagnetic Fields. Springer-Verlag, Berlin, 1993.